

Optical detection of ammonia in water using integrated up-conversion fluorescence in a fiberized microsphere

Meng Zhang, Ruoning Wang, Ke Tian, Jibo Yu, Gilberto Brambilla, Libo Yuan and Pengfei Wang

Abstract—A novel optical sensor for ammonia concentration in water is demonstrated using up-conversion (UC) fluorescence intensity ratio (FIR). The sensor element consists of (i) an Er^{3+} - Yb^{3+} co-doped tellurite glass microsphere integrated inside a section of suspended tri-core hollow fiber (STCHF) and (ii) the pH indicator phenol red. When 980 nm pump is coupled into the microsphere, the Er^{3+} ions produce green and red UC emissions. Exposure to ammonia results in a strong increase in the 560 nm absorption of the phenol red, which acts as a filter for the green emission, while the red emission is unaffected. A simple linear relation between the FIR and the ammonia aqueous concentration has been established.

Index Terms—Microsphere, up-conversion, optical ammonia sensor, integrated device.

I. INTRODUCTION

Ammonia is an important constituent in explosives, fertilizers, and industrial coolants, and can be very harmful even at very low concentrations [1, 2]: 22.8 ppm can be lethal to water organisms and exposure to ammonia as low as 35 ppm for over 15 min can be dangerous to humans [3, 4]. In the past decade, many types of ammonia sensors have been proposed based on electrochemical sensing, such as chemiresistors [5] and chemically modified field effect transistors [6]. These electrochemical methods have high selectivity and low detection limits, but have issues with lifetime, miniaturization and stability of the reference electrodes, which have a negative effect on practical applications. Optical ammonia sensors have attracted increased attention because of their advantages in selectivity, repeatability, portability, and immunity to electromagnetic interference [7-9]. Usually, optical ammonia sensors are based on absorbance or fluorescence emissions of ammonia-selective

dyes [10, 11]. For example, Tavoli et al. proposed a polypyrrole film doped with Eriochrome cyanine R to detect ammonia gas [12]: the sensor presented significant absorbance variations upon exposure to different ammonia gas concentrations at room temperature and exhibited fast response time and a low detection limit. Duong et al. reported an ammonia sensor based on FIR of a dye [13]: ethyl cellulose was combined with oxazine 170 perchlorate to form a thin membrane as sensing element: the FIR at 565 nm and 630 nm changed in different ammonia concentrations. In fact, ammonia is a weak base, thus can cause the pH to change, resulting in a change in color or fluorescence of the indicator dye [14, 15]. For example, UC nanoparticles can emit strong UC luminescence under near-infrared laser pumping [16, 17], which may correspond to the absorption band of some dyes, such as phenol red (PR). The UC luminescence intensity will be changed with the ammonia concentration change due to the strong absorption of PR [18].

To avoid complex synthesis of nanoparticles and/or of the indicator dye, here an Er^{3+} - Yb^{3+} co-doped tellurite glass microsphere is used as UC fluorescence emission medium. The microsphere is integrated inside a section of STCHF and fixed naturally so that the whole sensing structure is more compact and easier to connect with other fiber devices.

II. DEVICE FABRICATION AND SENSING PRINCIPLE

The STCHF used in these experiments, consisting of three 4 μm diameter suspended circular cores, an 80 μm diameter central air hole and a 125 μm outer diameter annular cladding (Fig. 1, left inset), was produced by YEOC, Inc. The Er^{3+} - Yb^{3+} co-doped tellurite glass ($72\text{TeO}_2 - 20\text{ZnO} - 5\text{Na}_2\text{CO}_3 - 1.5\text{Y}_2\text{O}_3 - 0.5\text{Er}_2\text{O}_3 - 1\text{Yb}_2\text{O}_3$), used for the microsphere, was prepared using a traditional melt-quenching method. The powdered PR (Aladdin, CAS number 143-74-8) was dissolved in deionized

This work was supported by the National Key program of Natural Science Foundation of China (NSFC 61935006, 62090062), Shenzhen Basic Research Project (JCYJ20190808173619062), the 111 project (B13015) to the Harbin Engineering University, Heilongjiang Touyan Innovation Team Program and The PhD Student Research and Innovation Fund of the Fundamental Research Funds for the Central Universities (3072021CF2501). (Corresponding author: Libo Yuan and Pengfei Wang.)

M. Zhang, R. Wang and J. Yu are with the Key Laboratory of In-Fiber Integrated Optics of Ministry of Education, College of Science, Harbin Engineering University, Harbin 150001, China (e-mail: mengzhang@hrbeu.edu.cn; ruoningwang@hrbeu.edu.cn; yu20131164@hrbeu.edu.cn).

K. Tian is with Okinawa Institute of Science and Technology Graduate University, Onna, Okinawa 904-0495, Japan (e-mail: ke.tian@oist.jp).

Gilberto Brambilla is with the Optoelectronics Research Centre, University of Southampton, Southampton SO17 1BJ, UK (e-mail: gilberto@soton.ac.uk).

L. Yuan is with the Photonics Research Center, Guilin University of Electronic Technology, Guilin, China (email: lbyuan@vip.sina.com).

P. Wang is with the Key Laboratory of In-Fiber Integrated Optics of Ministry of Education, College of Science Harbin Engineering University, Harbin 150001, China, and also with the Key Laboratory of Optoelectronic Devices and Systems of Ministry of Education and Guangdong Province, College of Optoelectronic Engineering, Shenzhen University, Shenzhen 518060, China. (email: pengfei.wang@tudublin.ie).

water and prepared into a 0.05% mass fraction solution for the further operations.

Figure 1 shows the schematic of the in-fiber integrated microsphere sensing structure used in our experiments. One end of the STCHF was spliced with a section of a multi-mode fiber (MMF) and then with a single-mode fiber (SMF) to maximize pump light coupling from the SMF into the suspended cores and reduce the overall transmission loss. The STCHF was then tapered down using a special fusion splicer to make the suspended cores thinner, thus enhance the evanescent field in the air hole, and form a conical region that can host the microsphere stable. Finally, the tapered STCHF was cut and a 50 μm diameter microsphere was placed into the STCHF air hole before the STCHF was spliced to a SMF to complete packaging. Figure 2 shows the step-by-step process to place the microsphere inside the hollow fiber.

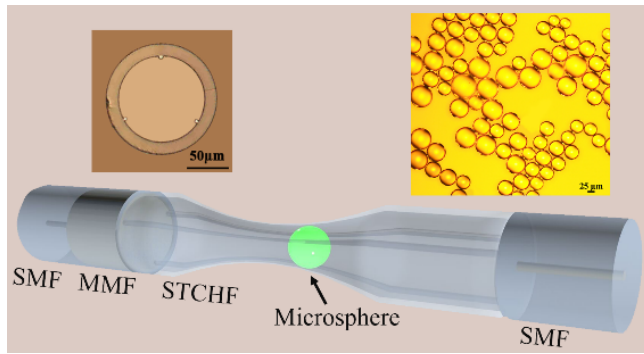


Fig. 1. Schematic of the integrated microsphere sensing structure; left inset: microscope image of the STCHF cross section; right inset: microscope image of the $\text{Er}^{3+}\text{-Yb}^{3+}$ co-doped tellurite glass microspheres prepared in our lab.

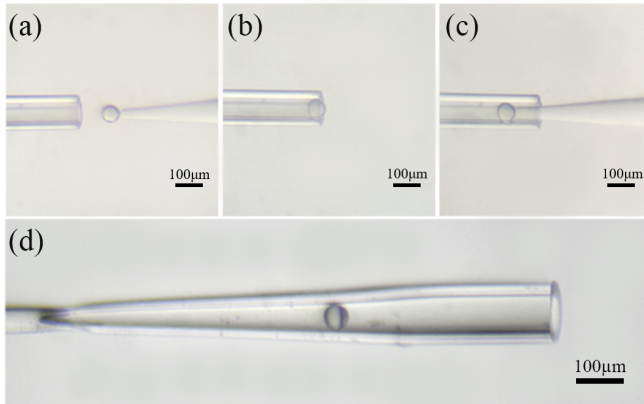


Fig. 2. Microscope images (a) – (d) of the process of microsphere transfer and placement.

The $\text{Er}^{3+}\text{-Yb}^{3+}$ co-doped tellurite glass microspheres were prepared by droplet method [19]: the bulk tellurite glass was ground into powders, which were then poured into a vertical furnace with an internal gas flow. At high temperature, the powders softened and became microspheres because of the action of the surface tension. The size of the microspheres can be changed by adjusting flow rate and temperature. Finally, a large number of microspheres were collected in a Petri dish attached to the end of a quartz tube. As shown in the right inset

of Fig. 1, the microspheres have uniform size, smooth surface and no contamination.

PR is nontoxic and not fluorescent when pumped in the near IR. The absorption spectra of PR at three typical pH values and the emission spectrum of the microsphere integrated inside hollow fiber were measured respectively. As shown in Fig. 3, for increasing pH values, the most prominent absorption band changes from 435 nm to 560 nm, which overlaps with the microsphere green emission band. The absorption wavelength shift is particularly pronounced for a pH change from 7 to 9: for increasing ammonia solution concentrations, the PR absorption at 560 nm increases, thus the microsphere green fluorescence emission is frustrated, while the red emission is largely unaffected, which can achieve the ammonia detection based on the relationship of FIR and ammonia concentration.

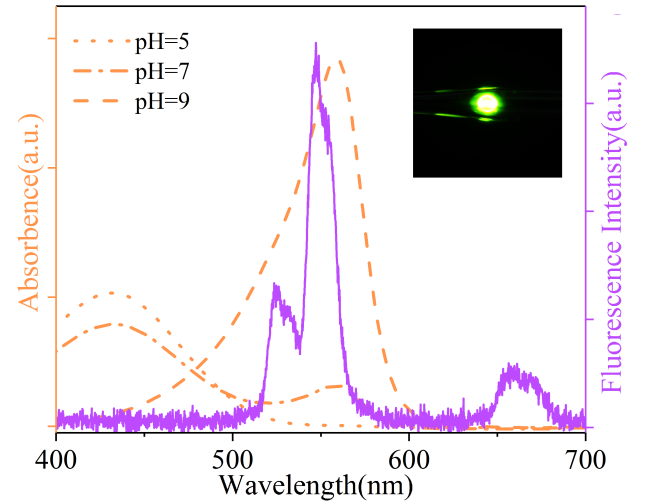


Fig. 3. Absorption spectra of PR at three typical pH values and emission spectrum of the microsphere integrated inside the hollow fiber. Inset: microscope image of the microsphere emission under 980nm pumping.

III. EXPERIMENTS AND DISCUSSION

Fig. 4 shows the set-up used for the ammonia detection experiments. The fiber sensing unit was placed inside a transparent sealed box and immersed in the PR solution. A small hole was made at the top of the sealing box with hole size matching the diameter of the dropper. A two-component epoxy adhesive was used to glue the dropper to the sealed box and fill the gap between the dropper and the hole to ensure good sealing. A 980 nm laser diode (MCSPL-980, MC Fiber Optics, China) was used to pump the $\text{Er}^{3+}\text{-Yb}^{3+}$ co-doped tellurite glass microsphere through the suspended cores. In order to avoid any influence of the liquid level change on the measurements, the spectrometer (USB4000, Ocean Optics, China) optical probe was fixed below the sealed box to collect the microsphere UC fluorescence and the emission spectrum was obtained by processing the collected signals using computer analysis software (Ocean Optics). When ammonia solution was continuously added through the dropper, the ratio of UC green to red emission was monitored.

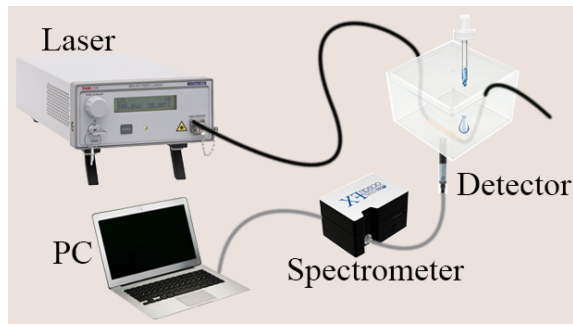


Fig. 4. Experiment setup for monitoring ammonia concentration in water.

The effect of PR solution on the microsphere UC luminescence in different pH environments was studied by fixing the STCHF integrated microsphere structure to the bottom of a petri dish, and placing above the microsphere the optical probe connected with a spectrometer to analyze and record the fluorescence spectra. A buffer solution with different pH values was dropped into the petri dish containing the sensing unit, and the UC fluorescence spectrum of the microsphere was recorded. Fig. 5(a) shows that the microsphere UC fluorescence emission is hardly affected by pH. Fig. 5(b) further proves that there is no significant difference in the intensities of green and red light and their ratio at different pH values. However, when PR solution is added into the buffer solution, the UC fluorescence emissions of the microsphere collected by the probe differs at different pH values, as shown in Fig. 5(c). When the solution pH value increases above 6, the microsphere green UC fluorescence emission detected by the probe begins to decrease, while the red signal remains nearly unchanged. The FIR as a function of pH is shown in Fig. 5(d), which illustrates that in weak base environments the PR has an impact on the microsphere UC fluorescence spectrum collected by the probe.

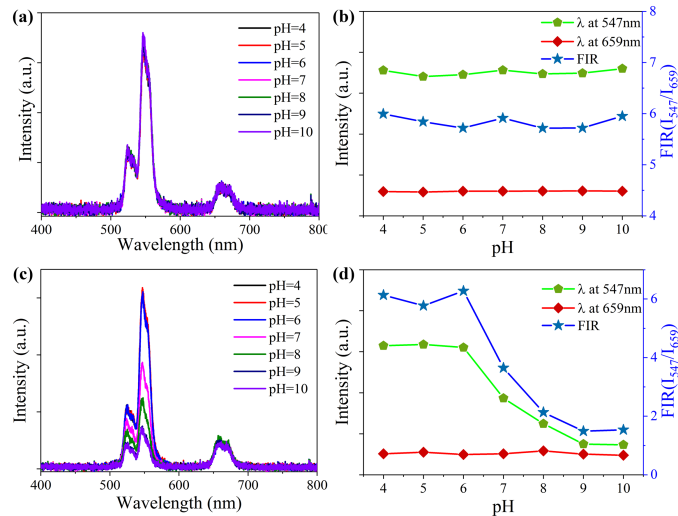


Fig. 5. (a,c) UC fluorescence spectra of the Er^{3+} - Yb^{3+} co-doped tellurite glass microsphere and (b,d) fluorescence peak intensity at 547 nm and 659 nm, and their ratio in different pH values buffer solutions without (a,b) and with (c,d) PR. The pump wavelength was 980 nm.

The fiberized integrated microsphere structure properties were characterized by using the experiment setup shown in Fig.

4. Ammonia solution with concentration ranging from 0 to 4 ppm was dropped into the sealed box. The laser pump power was chosen to minimize any possible thermal effects on fluorescence. For increasing ammonia concentrations, the green fluorescence emission gradually weakened due to the absorption of PR, while the red fluorescence intensity remained unchanged, as shown in Fig. 6(a). For increasing ammonia concentrations, the ratio of fluorescence intensity at 547 nm and 659 nm shows an exponential decrease. The absorption of green light by PR gradually reaches saturation. At low ammonia concentrations, the volatilization rate of ammonia is fast, resulting in an unstable FIR during the set measurement time. It was found that the UC luminescence spectra were not stable at ammonia concentrations lower than 0.5 ppm. Therefore, the limit of detection (LOD) of ammonia concentration in water was determined to be 0.5 ppm.

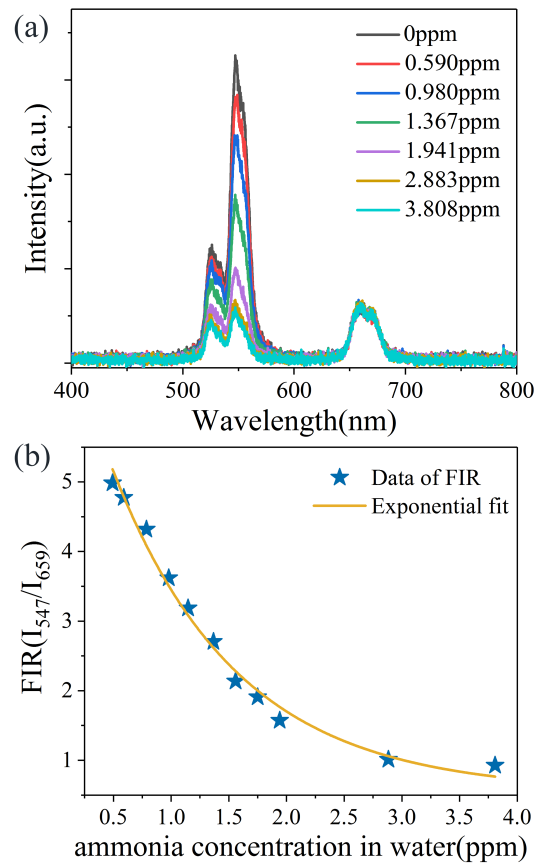


Fig. 6. (a) Collected UC fluorescence spectra of the Er^{3+} - Yb^{3+} co-doped tellurite glass microsphere in different ammonia concentration solutions; (b) relationship between FIR and ammonia concentration in water.

The response and recovery times of the sample sensor are shown in Fig. 7(a). The STCHF integrated microsphere sample was fixed at the bottom of petri dish. One end of multimode fiber was fixed above the microsphere to collect the UC fluorescence signal, while the other was connected to an oscilloscope to record the temporal signal changes. To distinguish the sensor response time from the diffusion time of ammonia in the PR solution, ready prepared solutions of ammonia in PR were used. The solutions were dropped into the petri dish for testing the response time and appropriate amounts of deionized water were added to dilute the ammonia solution

for testing the recovery time. The intrinsic response time and recovery times were found to be about 0.20 s and 0.25 s respectively. The short jitter observed at the rising and the falling edges is attributed to the instability of the light intensity caused by the liquid drop.

Sensor's repeatability and stability were checked by monitoring the UC fluorescence spectra of the STCHF integrated microsphere sample every second day. Great care was taken to ensure that the relative distance between the probe and the microsphere was constant, to avoid any effect on the fluorescence spectra. Fig. 7(b) shows that there is little difference in the fluorescence intensity at 547 nm and 659 nm, and in particular in their ratio, which illustrates that the STCHF integrated microsphere structure for ammonia detection has excellent repeatability.

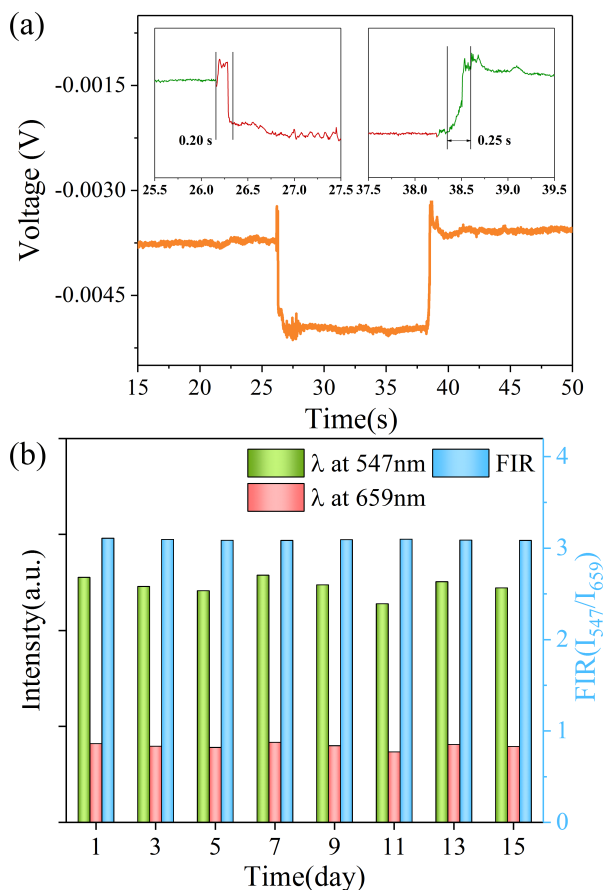


Fig. 7. (a) Response and recovery times and (b) repeatability of the STCHF integrated microsphere sample at room temperature.

IV. CONCLUSION

In conclusion, a sensor for aqueous ammonia solutions was proposed and demonstrated integrating a STCHF with an Er^{3+} - Yb^{3+} co-doped tellurite glass microsphere and PR. Under 980 nm laser pumping, the UC fluorescence emissions of the microsphere were obtained. Due to the increased absorption of PR at 560 nm in weak base environments, the green UC fluorescence of the microsphere was weakened when the sensor was exposed in ammonia. With increasing ammonia

concentrations in water, the fluorescence intensity at 547 nm gradually decreased while at 659 nm remained unchanged. For ammonia concentrations from 0 to 4 ppm, the FIR is exponentially dependent on the ammonia concentration. The sensor had a limit of detection of 0.5 ppm, a fast response time (<1 s) and excellent repeatability. The optical sensor based on FIR technology fabricated in this work is low-cost, versatile, and fast for sensing of ammonia concentrations in water.

REFERENCES

- [1] B. Timmer, W. Olthuis and A. V. D. Berg, "Ammonia sensors and their applications—a review", *Sensors & Actuators B Chemical*, vol. 107, no. 2, pp. 666-677, 2005.
- [2] V. Mahendran and J. Philip, "An optical technique for fast and ultrasensitive detection of ammonia using magnetic nanofluids", *Applied Physics Letters*, vol. 102, no. 6, pp. 5002-8879, 2013.
- [3] S. Paramasivam, K. Jayaraman, T. C. Wilson, A. K. Alva, L. Kelson and L. B. Jones, "Ammonia volatilization loss from surface applied livestock manure", *Journal of Environmental Science & Health Part B*, vol. 44, no. 3, pp. 317-324, 2009.
- [4] M. Pisco, M. Consales, S. Campopiano, A. Cutolo and A. Cusano, "Ammonia detection in water with a tin dioxide based optical sensor", *Proceedings of SPIE - The International Society for Optical Engineering*, vol. 5952, pp. 293-301, 2005.
- [5] Y. Li, Y.-Q. Liu, L.-W. Liu and G.-B. Pan, "Ammonia Chemiresistor Sensor Based on Poly(3-Hexylthiophene) Film Oxidized by Nitrosonium Hexafluorophosphate", *Chemistry Letters*, vol. 41, no. 12, pp. 1569-1570, 2012.
- [6] J. Yu, X. Yu, L. Zhang and H. Zeng, "Ammonia gas sensor based on pentacene organic field-effect transistor", *Sensors and Actuators B: Chemical*, vol. 173, pp. 133-138, 2012.
- [7] T. Tsuboi, Y. Hirano, Y. Shibata and S. Motomizu, "Sensitivity Improvement of Ammonia Determination Based on Flow-Injection Indophenol Spectrophotometry with Manganese(II) Ion as a Catalyst and Analysis of Exhaust Gas of Thermal Power Plant", *Analytical Sciences*, vol. 18, no. 10, pp. 1141-1144, 2002.
- [8] K. Waich, S. Borisov, T. Mayr and I. Klimant, "Dual lifetime referenced trace ammonia sensors", *Sensors and Actuators B: Chemical*, vol. 139, no. 1, pp. 132-138, 2009.
- [9] G. H. Mount, B. Rumburg, J. Havig, B. Lamb, H. Westberg, D. Yonge, K. Johnson and R. Kincaid, "Measurement of atmospheric ammonia at a dairy using differential optical absorption spectroscopy in the mid-ultraviolet", *Atmospheric Environment*, vol. 36, pp. 1799-1810, 2002.
- [10] A. H. Jalal, J. Yu and A. G. Agwu Nnanna, "Fabrication and calibration of Oxazine-based optic fiber sensor for detection of ammonia in water", *Applied Optics*, vol. 51, no. 17, pp. 3768-3775, 2012.
- [11] R. Claps, F. V. Englich, D. P. Leleux, D. Richter and R. F. Curl, "Ammonia Detection by use of Near-Infrared Diode-Laser-Based Overtone Spectroscopy", *Applied Optics*, vol. 40, no. 24, 4387-4394, 2001.
- [12] F. Tavoli and N. Alizadeh, "Optical ammonia gas sensor based on nanostructure dye-doped polypyrrole", *Sensors & Actuators B Chemical*, vol. 176, pp. 761-767, 2013.
- [13] D. J. I. Rhee, "A ratiometric fluorescence sensor for the detection of ammonia in water", *Sensors and Actuators B: Chemical*, vol. 190, pp. 768-774, 2014.
- [14] C. Preininger, G. J. Mohr, I. Klimant and O. S. Wolfbeis, "Ammonia fluorosensors based on reversible lactonization of polymer-entrapped rhodamine dyes, and the effects of plasticizers", *Analytica Chimica Acta*, vol. 334, no. 1-2, pp. 113-123, 1996.
- [15] I. M. Raimundo and R. Narayanaswamy, "Simultaneous determination of relative humidity and ammonia in air employing an optical fibre sensor and artificial neural network", *Sensors & Actuators B*, vol. 74, no. 1-3, pp. 60-68, 2001.
- [16] H. Huang, J. Chen, Y. Liu, J. Lin, and D. J. S. Chen, "Lanthanide-doped core multishell nanoarchitectures: multimodal excitable upconverting downshifting luminescence and high-level anti-counterfeiting ", *Small*, vol. 16, no. 19, p. 2000708, 2020.
- [17] J. Lin, C. Yang, P. Huang, S. Wang, and D. J. C. E. J. Chen, "Photoluminescence tuning from glass-stabilized CsPbX_3 ($\text{x}=\text{Cl}, \text{Br}, \text{I}$) perovskite nanocrystals triggered by upconverting Tm^{3+} : KYb_2F_7

- nanoparticles for high-level anti-counterfeiting", *Chemical Engineering Journal*, vol. 395, p. 125214, 2020.
- [18] H. S. Mader and O. S. Wolfbeis, "Optical Ammonia Sensor Based on Upconverting Luminescent Nanoparticles", *Analytical Chemistry*, vol. 82, no. 12, pp. 5002-5004, 2010.
- [19] G. R. Elliott, D. W. Hewak, G. S. Murugan and J. S. Wilkinson, "Chalcogenide glass microspheres; their production, characterization and potential", *Optics Express*, vol. 15, no. 26, pp. 17542-17553, 2007.